THE JOURNAL OF BIOLOGICAL CHEMISTRY VOL. 286, NO. 11, pp. 9555–9566, March 18, 2011

Phosphatidylinositol 3′-Kinase Activity Is Critical for Initiating the Oxidative Burst and Bacterial Destruction during CEACAM3-mediated Phagocytosis*[S]

Received for publication, December 23, 2010 Published, JBC Papers in Press, January 7, 2011, DOI 10.1074/jbc.M110.216085

Alexander Buntru[‡§1], **Kathrin Kopp**[‡1], **Maike Voges**[‡§], **Ronald Frank**[¶], **Verena Bachmann**[‡], **and Christof R. Hauck**[‡§2]

From the [‡]*Lehrstuhl für Zellbiologie and* [§]*Konstanz Research School Chemical Biology, Universität Konstanz, 78457 Konstanz and the* [¶]*Department of Chemical Biology, Helmholtz Centre for Infection Research, 38124 Braunschweig, Germany*

Carcinoembryonic antigen-related cell adhesion molecule 3 (CEACAM3) is an immunoglobulin-related receptor expressed on human granulocytes. CEACAM3 functions as a single chain phagocytotic receptor recognizing Gram-negative bacteria such as *Neisseria gonorrhoeae*, which possess CEACAM-binding adhesins on their surface. The cytoplasmic domain of CEACAM3 contains an immunoreceptor tyrosine-based activation motif (ITAM)-like sequence that is phosphorylated upon receptor engagement. Here we show that the SH2 domains of the regulatory subunit of phosphatidylinositol 3′-kinase (PI3K) bind to tyrosine residue 230 of CEACAM3 in a phosphorylation-dependent manner. PI3K is rapidly recruited and directly associates with CEACAM3 upon bacterial binding as shown by FRET analysis. Although PI3K activity is not required for efficient uptake of the bacteria by CEACAM3-transfected cells or primary human granulocytes, it is critical for the stimulated production of reactive oxygen species by infected phagocytes and the intracellular degradation of CEACAM-binding bacteria. Together, our results highlight the ability of CEACAM3 to coordinate signaling events that not only mediate bacterial uptake, but also trigger the killing of internalized pathogens.

The Gram-negative bacterium *Neisseria gonorrhoeae* (Ngo), the causative agent of gonorrhea, is a paradigm for antigenic and phase variation of surface components that allow escape from the acquired immune response of its sole natural host, the human (1, 2). One family of neisserial outer membrane proteins that is modulated by phase variation are the colony opacity associated (Opa) proteins (for review, see Ref. 3). There are up to 12 *opa* genes encoded on the gonococcal chromosome that are constitutively transcribed, but the expression of each Opa protein is independently controlled by pentameric sequence repeats in the 5′ coding region of each transcript. The number of these repetitive units determines if the full-length protein is translated or if, due to reading frameshifts and generation of a premature stop codon, a truncated, non-functional protein is made (4). Interestingly, most gonococcal Opa proteins characterized so far bind to various members of the carcinoembryonic antigen-related cell adhesion molecule (CEACAM)[3] family, a group of immunoglobulin-domain containing glycoproteins found on human cells (for review, see Ref. 5). CEACAMs harbor at least one characteristic immunoglobulin variable (Ig_V)-like amino-terminal domain that is recognized by CEACAM-binding Opa proteins (Opa_{CEA} proteins) (6, 7). Opa_{CEA} protein binding to the host receptor is a direct protein-protein interaction that is species-specific in the sense that Opa_{CEA} proteins only recognize human CEACAMs, but not orthologues from other mammals (8). Moreover, of the 12 CEACAM family members expressed in humans (9), only four have been found to associate with gonococcal Opa_{CEA} proteins, namely CEACAM1, CEACAM3, CEA (the product of the *CEACAM5* gene), and CEACAM6 (10–14). The situation is further complicated by the fact that most CEACAM-binding Opa proteins characterized to date bind to CEA and CEACAM1 only (*e.g.* Opa_{56} of strain MS11), whereas a few other Opa_{CEA} proteins (such as Opa_{52} of strain MS11) associate with all four Opa-binding CEACAMs including CEACAM3 (12, 15, 16). This striking misbalance of CEACAM-binding properties can be best reconciled by looking at the tissue distribution of human CEACAMs: CEACAM1, CEA, and CEACAM6 are found on the apical membrane of polarized epithelia, where these receptors are exploited by pathogenic *Neisseriae* for colonizing the mucosal surface (17, 18). In contrast, CEACAM3 is exclusively expressed by human granulocytes and acts as an efficient, opsonin-independent phagocytic receptor for CEACAM-binding bacteria (reviewed in Ref. 19). Therefore, it has been speculated that despite their antigenic variation and escape from the acquired immune system, these bacteria can be controlled by human innate immune cells that recognize the CEACAM-binding properties of the microbes by the help of CEACAM3. Not surprisingly, bacterial uptake via CEACAM3 is more efficient and mechanistically distinct from bacterial internalization via the epithelial CEACAMs (CEACAM1, CEA, and CEACAM6) (20, 21). Epithelial CEACAMs mediate endocytosis of bound particles by a process that does not require cytoplasmic determinants of these receptors, but depends on

* This work was supported by Landesstiftung BW (LS-Prot-66) and a grant from the Ministry of Science, Research and the Arts of Baden-Württemberg (to C. R. H.).

[S] The on-line version of this article (available at http://www.jbc.org) contains supplemental Fig. S1.

[1] Both authors contributed equally to this work.

[2] To whom correspondence should be addressed: Postfach X908, 78457 Konstanz, Germany. Tel.: 49-0-7531-88-2286; Fax: 49-0-7531-88-2149; E-mail: christof.hauck@uni-konstanz.de.

[3] The abbreviations used are: CEACAM, carcinoembryonic antigen-related cell adhesion molecule; PTK, protein-tyrosine kinase; ITAM, immunoreceptor tyrosine-based activation motif; m.o.i., multiplicity of infection; SH, Src homology; PI(3,4,5)P, phosphatidylinositol 3,4,5-trisphosphate; PI3P, phosphatidylinositol 3-phosphate.

cholesterol- and sphingolipid-rich membrane microdomains (21, 22). In contrast, cholesterol depletion does not affect CEACAM3-mediated phagocytosis by human granulocytes, but the cytoplasmic domain of CEACAM3 is critical for this process (21, 23). Combined biochemical, mutational, and functional studies have shown that CEACAM3 engagement by Opa_{CEA} protein-expressing bacteria triggers the phosphorylation of tyrosine residues within the cytoplasmic domain of CEACAM3 by Src family protein-tyrosine kinases (PTKs) that transiently associate with CEACAM3 during bacterial uptake (21, 24–26). The phosphorylated tyrosine residues are embedded in an amino acid context that resembles an immunoreceptor tyrosine-based activation motif (ITAM). Therefore, it has been speculated that CEACAM3 functions analogous to the well studied Fcγ receptors (FcγR) that mediate uptake of antibody-opsonized particles (27). Although there are similarities with regard to the involvement of Src family PTKs, CEACAM3 seems to be connected in a different manner to downstream signaling components. For example, coexpression of the tyrosine kinase Syk can enhance FcγR-mediated uptake in transfected cell lines, whereas Syk co-expression does not increase CEACAM3-mediated uptake of *N. gonorrhoeae* (28, 29). Furthermore, one of the tyrosine residues within the ITAM-like sequence of CEACAM3 (tyrosine residue 230; Tyr^{230}) serves as a docking site for the guanine nucleotide exchange factor Vav, a situation not observed for FcγR (30, 31). Direct binding of Vav via its SH2 domain to phospho-Tyr^{230} explains the strong stimulation of the small GTPase Rac that is observed in primary granulocytes and CEACAM3-expressing cell lines upon infection with Opa protein-expressing gonococci (23, 24). Exchange of CEACAM3 Tyr^{230} for phenylalanine, genetic deletion of Vav1 and Vav2, or interference with Rac stimulation impair CEACAM3-mediated uptake (23, 30). Mutation of the second tyrosine residue within the CEACAM3 ITAM-like sequence, Tyr^{241}, also results in reduced phagocytosis of Opa protein-expressing gonococci (23, 25). This residue is located in the context of a Y*XX*M motif that is known to serve as a high affinity recognition site for the SH2 domain of the phosphatidylinositol 3′-kinase class I (PI3K) regulatory subunit (32). In contrast to class II and class III enzymes, PI3Ks are heterodimers composed of one p85 or p50–55 regulatory subunit and one of three possible catalytic subunits (p110 α, β, or γ). They are activated by different types of cell-surface receptors and generate the lipid phosphatidylinositol 3,4,5-trisphosphate (PI(3,4,5)P), which can be recognized by a variety of effector proteins (33). Indeed, PI(3,4,5)P accumulates during internalization of Opa_{CEA} protein-expressing *N. gonorrhoeae* by CEACAM3-expressing HeLa cells (34). However, it is currently not known if PI3K is recruited to CEACAM3 upon bacterial binding and if this lipid kinase directly or indirectly associates with the CEACAM3 cytoplasmic domain.

In this study, we reassess the involvement of PI3K in CEACAM3-mediated uptake of *N. gonorrhoeae* using transiently transfected cells and primary human granulocytes. Biochemical and microscopic approaches demonstrate that the SH2 domains of the regulatory subunit of PI3K directly associate with the cytoplasmic domain of CEACAM3. Unexpectedly, this association takes place at Tyr^{230}, and does not involve the Y*XX*M motif surrounding Tyr^{241}. Importantly, pharmacological inhibition of PI3K activity does not interfere with CEACAM3-mediated uptake by transfected cell lines or primary human granulocytes, but selectively blocks the generation of reactive oxygen species by phagocytes and the resulting destruction of the bacteria. These data suggest that CEACAM3-expressing innate immune cells can specifically detect and eliminate CEACAM3-binding pathogens by an opsonin-independent process.

EXPERIMENTAL PROCEDURES

Recombinant DNA Constructs—Mammalian expression vectors encoding the HA-tagged versions of CEACAM3 (23) were used as template for amplification with primers CEACAM3-IF-sense, 5′-GAAGTTATCAGTCGATACCATGGGGCCCCCCTCAGCC-3′, and HA-CEACAM-IF-antisense, 5′-ATGGTCTAGAAAGCTTGCAGCGTAATCTGGAACGTCATATGG-3′. The resulting PCR fragments were cloned into pDNR-Dual using the In-Fusion PCR Cloning Kit (Clontech) and transferred by Cre-mediated recombination into pLPS-3′EGFP (Clontech) resulting in GFP fused to the carboxyl terminus of the expressed proteins. Similarly, HA-tagged CEACAM1–4L in pDNR-Dual was transferred to pLPS-3′mKate (18, 22). CyPet-tagged CEACAM3, pYPet loxP, and pmKate loxP as well as the v-Src encoding construct were described previously (26, 35). cDNA clones for different human SH2 domain containing proteins were obtained from ImaGenes (Berlin, Germany). The SH2 domains of PI3K regulatory subunit γ (PI3K) were amplified from full-length cDNA (clone IRATp970D0537D6) by PCR with primers for the N-terminal SH2 domains PI3KR3-N-SH2-IF-sense, 5′-GAAGTTATCAGTCGACATGAAGGACAGTTCTGTTTC-3′, and PI3KR3-N-SH2-IF-antisense, 5′-ATGGTCTAGAAAGCTTAATCCTGTTGGTATCTGGAC-3′, and for C-terminal SH2 domains PI3KR3-C-SH2-IF-sense, 5′-GAAGTTATCAGTCGACGAGGAAGATGAAAACCTGCC-3′, and PI3KR3-C-SH2-IF-antisense, 5′-ATGGTCTAGAAAGCTTATCTGCAAAGCGAGGGCATC-3′. The resulting PCR fragments were cloned into pDNR-Dual using the In-Fusion PCR Cloning Kit (Clontech). The SH2 domains of PI3K and all other SH2 domains were cloned and expressed as GST fusion proteins in *Escherichia coli* BL21 as described previously (21, 30). The N-terminal SH2 domain of PI3K and the SH2 domains of Hck and Slp76 were transferred from pDNR-Dual into pmKate loxP or pYPet loxP by Cre/lox recombination.

Cell Culture, Transfection of Cells, Cell Lysis, and Western Blotting—The human embryonic kidney cell line 293T (293 cells) was grown in DMEM supplemented with 10% calf serum at 37 °C, 5% CO_2. Murine macrophages (Raw 264.7) were cultured in RPMI 1640 with 10% heat-inactivated fetal calf serum (FCS) at 37 °C, 5% CO_2. Both cell lines were subcultured every 2–3 days. Transfection with expression vectors was accomplished by standard calcium-phosphate co-precipitation using a total amount of 6 μg of plasmid/10-cm culture dish. Cells were used 2 days after transfection. Primary human granulocytes were isolated from freshly drawn blood as described previously (23). In some experiments cells were treated 30 min prior to infection with wortmannin or LY294002 (Calbiochem,

San Diego, CA). Cell lysis and Western blotting were performed as described previously (35).

Bacteria—Non-piliated *N. gonorrhoeae* MS11-B2.1 strains expressing different CEACAM-binding Opa proteins (Opa_{52}, binding to CEACAM1, CEACAM3, CEA, and CEACAM6, strain N309; Opa_{56}, binding to CEACAM1 and CEA, strain N308) and the non-opaque strain N302 were described previously (23, 36) and were kindly provided by T. F. Meyer (Max-Planck-Institut für Infektionsbiologie, Berlin, Germany). The plasmid-based Opa proteins of these strains were sequence verified to correspond to the sequences reported by Kupsch *et al.* (36). Bacteria were grown on GC agar (Invitrogen) supplemented with vitamins at 37 °C, 5% CO_2, and subcultured daily. For labeling, bacteria (2×10^8/ml) were washed with sterile PBS and suspended in 0.5 μg/ml of 5-(6)-carboxyfluorescein succinimidyl ester (fluorescein), 4 μg/ml of Pacific Blue-NHS, or 4 μg/ml of Alexa Fluor 647 (AF647)-NHS (Invitrogen) in PBS. Suspensions were incubated at 37 °C for 30 min in the dark under constant shaking. Afterward bacteria were washed three times with PBS. Bacteria were Ig-opsonized with heat-inactivated rabbit antiserum diluted 1:2 in PBS for 1 h at 4 °C under constant overhead rotation. Prior to use, bacteria were washed in PBS. For infection, overnight grown bacteria were taken from GC agar plates, suspended in PBS, and colony forming units were estimated by OD_{550} readings according to a standard curve.

Antibodies and Reagents—Monoclonal antibody (mAb) against the GST tag (clone B-14) was from Santa Cruz Biotechnology (Santa Cruz, CA), mAb against v-Src (clone EC10) and against phosphotyrosine (clone 4G10) were from Upstate Biotechnology (Lake Placid, NY), mAb against GFP (clone JL-8) was from Clontech, and mAb against HA tag (clone 16B12) was purchased from Babco (Berkeley, CA). The monoclonal anti-Opa protein antibody (clone 4B12/C11) was a generous gift of Marc Achtman (MPI für Infektionsbiologie, Berlin, Germany). The rabbit polyclonal antibody against PI3K was from Upstate Biotechnology. A rabbit polyclonal antibody was generated against formaldehyde-fixed *N. gonorrhoeae* and *Neisseria meningitidis* (IG-511) by Immunoglobe (Himmelstadt, Germany). The IG-511 rabbit serum was heat inactivated at 56 °C for 1 h prior to use in bacterial opsonization.

Immunofluorescence Staining and Confocal Microscopy—Immunofluorescence staining was performed as described (21). Colocalization experiments and FRET acceptor bleaching studies were accomplished as described previously using a TCS SP5 confocal laser scanning microscope (Leica, Wetzlar, Germany) (26).

ELISA-based Interaction Assay—Plates were coated with 0.5 μg/well of GST fusion proteins or GST in PBS, pH 7.4, blocked overnight with 1% BSA in PBS containing 0.01% Tween (PBS-T), and incubated with equal amounts of diluted CEACAM3-containing or control whole cell lysates (overnight at 4 °C). CEACAM3 was detected by monoclonal anti-HA antibody followed by peroxidase-coupled goat anti-mouse antibody. TMB solution (0.5 mM 3,3′,5,5′-tetramethylbenzidine in 0.5% acetone, 4.5% ethanol, and 1 mM H_2O_2 in 30 mM potassium citrate, pH 4.1) was added, the reaction was stopped after 5 min with 2 M H_2SO_4, and absorbance was measured at 450 nm.

GST Pulldown Assay and Far Western Probing of Peptide Spot Membranes—For GST pulldown assays, 5 μg of purified GST or GST fusion proteins attached to glutathione-Sepharose beads (Amersham Biosciences) were added to 750 μl of cleared lysates from HEK293 cells transfected with CEACAM-encoding constructs or the empty vector (6 μg). Where indicated, the cells were additionally co-transfected with a v-Src-encoding plasmid (0.5 μg) to ensure maximal tyrosine phosphorylation of CEACAM3. Samples were incubated overnight at 4 °C under constant rotation. After four washes with PBS-T, precipitates were boiled in 2× SDS sample buffer before SDS-gel electrophoresis and Western blot analysis. Generation and probing of peptide spot membranes was conducted as described previously using 20 μg of GST-PI3K-N-SH2 or GST alone (30).

FRET Measurements—Measurements, including acceptor photobleaching, were done essentially as described (26). For FRET measurements in cell lysates, HEK293 cells were lysed 2 days after transfection and fluorescence intensities in the lysates were detected using a Varioskan Flash (ThermoScientific, Waltham, MA): donor channel (excitation/emission, 435 nm/477 nm), acceptor channel (excitation/emission, 500 nm/530 nm), and FRET channel (excitation/emission, 435 nm/530 nm). FRET was calculated by the following formula: $E_{A(\mathrm{app})} = (\mathrm{DA} - \alpha{\cdot}\mathrm{DD} - \beta{\cdot}\mathrm{AA})/\mathrm{AA}$ (DA, donor excitation/acceptor emission; DD, donor excitation/donor emission; AA, acceptor excitation/acceptor emission). The correction factors α and β were derived from samples expressing the donor or acceptor constructs only. For flow cytometric evaluation of FRET, samples were analyzed on a LSRII flow cytometer (BD Biosciences). Therefore, co-transfected cells were identified on the basis of donor and acceptor fluorescence and the fluorescence intensity in the FRET channel of these cells was determined. Cells expressing donor or acceptor constructs only were used to compensate for spectral bleed-through and cross-excitation.

Gentamicin Protection Assay—Assays were performed as described previously (22). Briefly, cells were seeded in 24-well plates coated with fibronectin (4 μg/ml) with 4×10^5 cells/well. A multiplicity of infection (m.o.i.) of 25 bacteria per cell was routinely used, and after 1 h of infection, extracellular bacteria were killed by a 45-min incubation in 50 μg/ml of gentamicin in DMEM. Then, cells were lysed with 1% saponin in PBS for 15 min. The samples were diluted with PBS, and the number of viable bacteria was determined by plating suitable dilutions on GC agar.

Quantification of Granulocyte Phagocytosis—Phagocytosis was determined by flow cytometry as described previously (37). Briefly, 1×10^6 granulocytes were incubated for 30 min at 37 °C with or without inhibitor. Granulocytes were infected with 2×10^7 fluorescein-labeled bacteria in 1 ml of phagocytosis buffer (PB; 1× PBS, 0.9 mM $CaCl_2$, 0.5 mM $MgCl_2$, 5 mM glucose, 1% heat-inactivated calf serum) for 15–30 min at 37 °C. Phagocytosis was stopped by the addition of ice-cold PB and samples were washed with PBS. Finally, samples were taken up in PBS, 1% heat-inactivated FCS, 2 mg/ml of trypan blue and analyzed on a LSRII. The percentage of fluorescein-positive cells was multiplied by the mean fluorescence of these cells to obtain an

estimate of the total amount of phagocytosed bacteria (uptake index).

Oxidative Burst Measurements—2×10^5 granulocytes were suspended in chemiluminescence buffer (8 g/liter of NaCl, 0.2 g/liter of KCl, 0.62 g/liter of KH_2PO_4, 1.14 g/liter of Na_2HPO_4, 1 g/liter of glucose, 50 mg/liter of bovine serum albumin, pH 7.2) and preincubated with the indicated concentrations of wortmannin for 30 min at 37 °C. Granulocytes were transferred to a 96-well plate in triplicate and luminol was added to a final concentration of 20 μg/ml. Samples were infected with 1×10^7 bacteria or left uninfected. PMA (1 μg/ml) was used as a positive control for oxidative burst. Chemiluminescence was determined every 2 min at 37 °C with a Varioskan Flash. To determine the total oxidative burst the response curves were exported to ImageJ and the areas under the curves were calculated.

Bacterial Degradation Assay—5×10^5 granulocytes were suspended in phagocytosis buffer and infected with 5×10^5 bacteria for 60 and 240 min at 37 °C under constant rotation in the presence or absence of wortmannin. Samples were centrifuged and cells were resuspended in 2× SDS sample buffer followed by gel electrophoresis and Western blot analysis.

RESULTS

The N-terminal SH2 Domain of PI3K Is Recruited to CEACAM3 Upon Infection with CEACAM3-binding Bacteria—Class I PI 3-kinases are critical for phagocytosis of opsonized particles by FcγR of murine macrophages and have been implicated in the uptake of bacteria via CEACAM3 (34, 38). We wanted to analyze how class I PI3Ks were mechanistically connected to CEACAM3-mediated uptake of Opa_{52}-expressing *N. gonorrhoeae*. Therefore, we transfected HEK293 cells with GFP-tagged wild type CEACAM3 (CEACAM3 WT-GFP) or a truncated CEACAM3 variant lacking the cytoplasmatic domain (CEACAM3 ΔCT-GFP) together with the N-terminal SH2 domain of the regulatory subunit γ of class I PI3K fused to mKate (mKate-PI3K-N-SH2). Furthermore, we co-transfected CEACAM3 with the SH2 domain of the Src family protein-tyrosine kinase Hck (mKate-Hck-SH2), which has been shown previously to co-localize and physically associate with CEACAM3 (21, 24, 26). Indeed, mKate-Hck-SH2 was strongly recruited to CEACAM3 at sites of bacteria-host cell contact (Fig. 1*A*). Similarly, mKate-PI3K-N-SH2 strongly colocalized with CEACAM3 in cells infected with the Opa_{52} protein expressing *N. gonorrhoeae* (Fig. 1*A*). In contrast, recruitment of PI3K-N-SH2 was absent in cells expressing CEACAM3 ΔCT-GFP, even though this mutated receptor containing a deletion of the complete cytoplasmatic domain was able to engage bacteria (Fig. 1*A*). To analyze if PI3K-N-SH2 is associated constitutively with CEACAM3, we infected cells with non-opaque gonococci that are not able to bind this receptor. Clearly, only a few cell-associated bacteria could be detected and the PI3K SH2 domain was not concentrated at sites of bacteria-host cell contact in this case (Fig. 1*A*). These results suggest that PI3K recruitment to CEACAM3 occurs in response to receptor stimulation. As a further control to investigate the specificity of SH2 domain recruitment to CEACAM3 in transfected cells we co-expressed the mKate-tagged SH2 domain of Slp76, which does not interact with CEACAM3 in biochemical assays (21). Indeed, the SH2 domain of Slp76 was not recruited to CEACAM3-bound gonococci (Fig. 1*A*). On average, about 8 bacteria were found to associate with each CEACAM3-transfected cell after 30 min, when the cells were infected at an m.o.i. of 30 (Fig. 1*B*). Whereas ~70% of the cell associated, CEACAM3-binding bacteria colocalized with the PI3K SH2 domain at this time point, none co-localized with the Slp76 SH2 domain (Fig. 1*B*). Together, these results supported the idea that class I PI3Ks are specifically recruited to the cytoplasmic domain of CEACAM3 upon receptor engagement by bacteria.

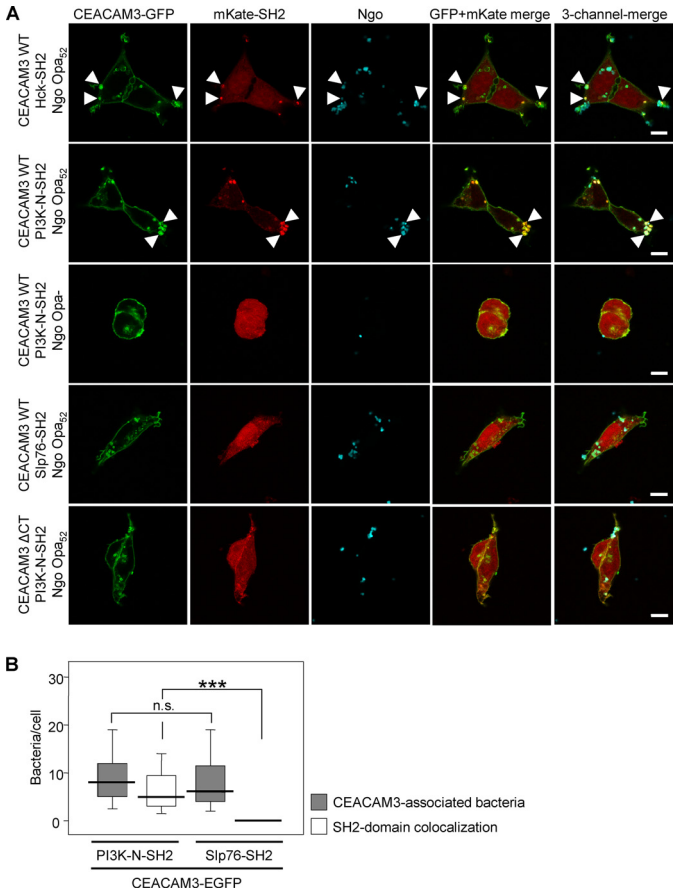

FIGURE 1. **N-terminal SH2 domain of class I PI 3-kinase is recruited to CEACAM3 upon infection with CEACAM3-binding gonococci.** *A*, HEK293 cells were cotransfected with expression plasmids coding for GFP-tagged wild type CEACAM3 (*CEACAM3 WT*) or a truncated CEACAM3 without cytoplasmic domain (*CEACAM3 ΔCT*) together with the indicated mKate-tagged SH2 domains derived from the PI3K regulatory subunit 3 (*PI3K*), the Src family PTK Hck, or Slp76, respectively. Cells were infected with Pacific Blue-labeled Opa_{52} protein-expressing (*Ngo* Opa_{52}) or non-opaque (*Ngo Opa*−) *N. gonorrhoeae* at m.o.i. 30 for 30 min, fixed, and analyzed by confocal microscopy. Recruitment of the SH2 domain to the clustered receptor is indicated by *white arrowheads*. *Scale bars*, 10 μm. *B*, HEK293 cells co-transfected with CEACAM3 WT-GFP and either mKate-PI3K-N-SH2 or mKate-Slp76-SH2 were infected with Ngo Opa_{52} as in *A*, and cell-associated bacteria co-localizing with CEACAM3-GFP were enumerated for 20 infected cells in each sample (*dark boxes*). At the same time, the co-localization of these cell-associated bacteria with the mKate2-labeled SH2 domains was evaluated (*white boxes*). *Boxes* represent the median (*thick line*), 25/75 (*boxes*), and 10/90 (*error bars*) percentiles of co-localizing bacteria in the samples. Statistical significance was evaluated by Wilcoxon's signed rank test ($n = 20$). *n.s.*, not significant; ***, $p < 0.001$.

PI3K-SH2 Domains Associate with the Cytoplasmatic Domain of CEACAM3—To investigate the biochemical basis of PI3K association with CEACAM3 we assayed the protein-pro-

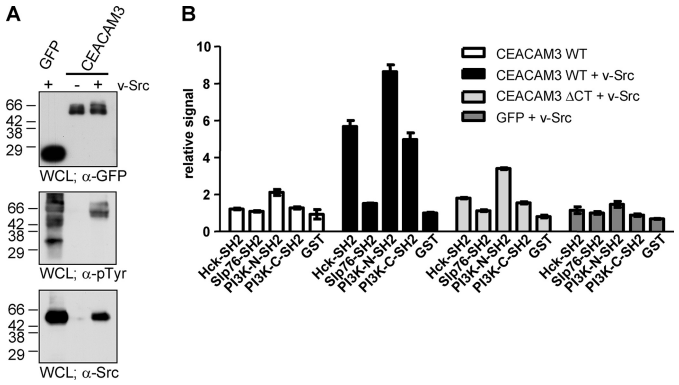

FIGURE 2. **Phosphorylated CEACAM3 associates with the SH2 domains of PI3K.** *A*, HEK293 cells were cotransfected with the empty control vector (*GFP*) or a vector encoding GFP-tagged wild type CEACAM3 together or not with v-Src. Equal amounts of whole cell lysates (*WCL*) were separated by SDS-PAGE and analyzed by Western blotting with monoclonal anti-GFP, anti-phosphotyrosine (*pTyr*) (*middle*), or anti-v-Src (*bottom*) antibodies. *B*, the indicated recombinant GST-SH2 domains or GST alone were coated in 96-well plates and incubated with whole cell lysates of cells expressing an HA-tagged GFP-fusion protein of wild type CEACAM3 (*CEACAM3 WT*) or a truncated CEACAM3 version lacking the cytoplasmic domain (*CEACAM3 ΔCT*) together or not with v-Src. As negative control, cell lysates co-expressing GFP and v-Src were used. Bound HA-tagged CEACAM3 wild type or CEACAM3 ΔCT were detected by monoclonal anti-HA antibody in an ELISA-based interaction assay. *Error bars* represent mean ± S.D. of triplicates.

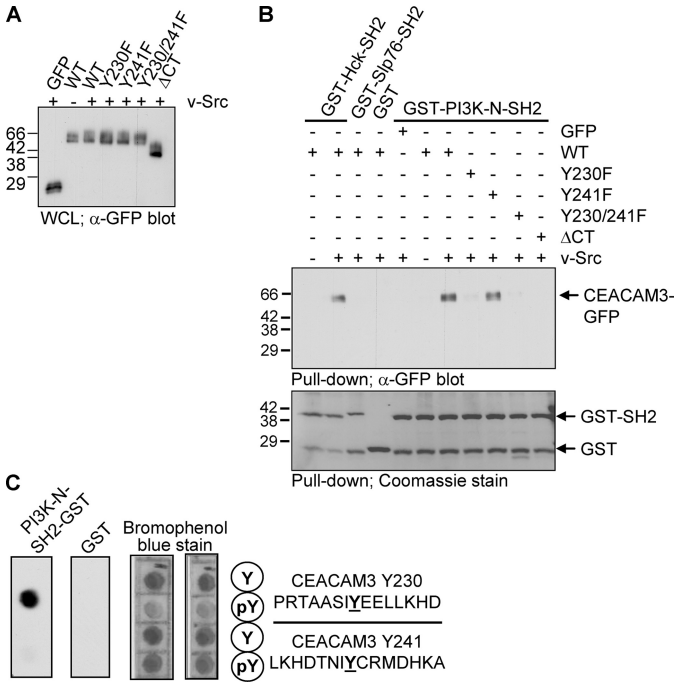

FIGURE 3. **The N-terminal domain of PI3K directly binds to phosphorylated Tyr^{230} of the CEACAM3 ITAM-like sequence.** *A*, HEK293 cells were transfected with the empty control vector (*GFP*) or constructs encoding the indicated GFP-tagged CEACAM3 variants wild type (*WT*), Y230F, Y241F, Y230F/Y241F, and ΔCT together or not with v-Src. Whole cell lysates (*WCL*) were analyzed for equal expression of CEACAM3 constructs. *B*, lysates from *A* were used in pulldown assays with the indicated GST fusion proteins or GST and detected with a monoclonal anti-GFP antibody (*upper panel*). Equal amounts of the GST fusion protein used in the pulldown assay were verified by Coomassie staining of the membrane (*lower panel*). *C*, peptide spot membranes harboring synthetic 15-mer peptides surrounding the indicated tyrosine residues of the CEACAM3 cytoplasmic domain (as indicated) in the unphosphorylated (*Y*) or tyrosine-phosphorylated (*pY*) forms were probed with GST-PI3K-N-SH2 or GST. Bound GST fusion proteins were detected with monoclonal anti-GST antibody (*left panels*). Immobilized synthetic peptides were visualized by bromphenol blue staining (*right panels*).

tein interaction by a solid phase binding assay. Therefore, CEACAM3 WT-HA-GFP, CEACAM3 ΔCT-HA-GFP, or GFP alone were expressed in HEK293 cells in the presence or absence of v-Src and cell lysates were generated. The presence of v-Src, an oncogene with constitutive protein-tyrosine kinase activity, results in strong, stimulation-independent tyrosine phosphorylation of CEACAM3. Indeed, Western blotting confirmed that CEACAM3 was expressed and tyrosine phosphorylated in the presence of v-Src (Fig. 2*A*). SH2 domains derived from the regulatory subunit of PI3K (PI3K-N-SH2 and PI3K-C-SH2), Hck (Hck-SH2), and Slp76 (Slp76-SH2) were expressed as GST fusions in *E. coli*, purified, and equal amounts were immobilized in 96-well plates. In addition, GST alone served as negative control. GST fusion proteins in each well were incubated with equal amounts of CEACAM3 WT-HA-GFP-, CEACAM3 ΔCT-HA-GFP-, or GFP-containing lysates. Following washing, the bound receptor was detected by a monoclonal anti-HA tag antibody (Fig. 2*B*). Importantly, unphosphorylated CEACAM3 did not associate with any SH2 domain, whereas v-Src-phosphorylated CEACAM3 strongly bound to the amino-terminal and carboxyl-terminal SH2 domains of PI3K as well as to the SH2 domain of Hck (Fig. 2*B*). SH2 domain binding was mediated by the cytoplasmic domain, because CEACAM3 ΔCT expressed in the presence of v-Src only showed background binding to SH2 domains (Fig. 2*B*). These results suggest that both SH2 domains of PI3K can physically associate with the tyrosine-phosphorylated cytoplasmic domain of CEACAM3.

PI3K-N-SH2 Binds to Phosphorylated Tyr^{230} within the Cytoplasmic Domain of CEACAM3—The cytoplasmic domain of CEACAM3 contains two tyrosine residues embedded within an ITAM-like sequence that has been shown to be critical for the function of this phagocyte receptor (21, 23, 30). To identify the tyrosine residue(s) within the CEACAM3 ITAM-like sequence, which are responsible for PI3K-N-SH2 binding, HEK293 cells were cotransfected with a v-Src-encoding plasmid together with a control vector (GFP), CEACAM3 WT, or several CEACAM3 mutants. The CEACAM3 mutants either exhibited a phenylalanine substitution of single tyrosine residues within the ITAM-like sequence (CEACAM3 Y230F and CEACAM3 Y241F), substitutions of both tyrosine residues (CEACAM3 Y230F/Y241F), or lacked the complete cytoplasmic domain (CEACAM3 ΔCT). The wild type and mutated receptors were present in cell lysates at similar levels (Fig. 3*A*). Using GST fusion proteins of SH2 domains derived from Hck, Slp76, PI3K, or using GST alone, pulldown assays were conducted with CEACAM3-containing lysates. Clearly, the Hck-SH2 domain was able to precipitate CEACAM3 WT upon phosphorylation by v-Src, whereas the Slp76 SH2 domain could not precipitate CEACAM3 (Fig. 3*B*). Similarly, the amino-terminal SH2 domain of PI3K was able to pull-down CEACAM3 WT as well as CEACAM3 Y241F from the lysates (Fig. 3*B*). In contrast, mutation of Tyr^{230} abrogated the association between CEACAM3 and PI3K-N-SH2 (Fig. 3*B*). Accordingly, mutation of both Tyr^{230} and Tyr^{241} as well as complete deletion of the CEACAM3 cytoplasmic domain also abolished this interaction (Fig. 3*B*) consistent with the view that binding of

the SH2 domain of PI3K occurs via the phosphorylated Tyr^{230} residue in the cytoplasmic domain of CEACAM3.

PI3K-N-SH2 Directly Associates with Phosphorylated CEACAM3 Tyr^{230}—SH2 domain-mediated binding to proteins from cell lysates can be due to indirect protein-protein interactions. To analyze whether PI3K-N-SH2 binds directly to CEACAM3 and whether this binding is independent of additional cellular components, we investigated the interaction of both molecules in a recombinant-synthetic combination. Therefore, 15-mer peptides encompassing each of the two tyrosine residues within the CEACAM3 ITAM-like sequence were synthesized as individual spots on a cellulose membrane (Fig. 3*C*) (39). Each peptide was produced in the unphosphorylated (Tyr) or the phosphorylated form (Tyr(P)). Subsequently, the membrane was incubated with GST-PI3K-N-SH2 or GST alone. The GST-PI3K-N-SH2 selectively bound to the phosphorylated peptide containing Tyr^{230} ($Tyr(P)^{230}$) of CEACAM3, whereas there was no binding to the same peptide in the unphosphorylated form (Fig. 3*C*). In line with the pull-down assays with CEACAM3 mutants, the SH2 domain of PI3K did not bind the peptide encompassing Tyr^{241} irrespective of the phosphorylation status of this tyrosine residue (Fig. 3*C*). Furthermore, there was no binding of the control protein (GST) to any of the peptides detectable (Fig. 3*C*). These results demonstrate that the PI3K-N-SH2 domain can directly and specifically bind to phosphorylated residue Tyr^{230} within the ITAM-like sequence of CEACAM3.

PI3K-N-SH2 Directly Binds to CEACAM3 in Intact Cells—The previous results demonstrate a specific association of the SH2 domain of PI3K with the phosphorylated cytoplasmatic domain of CEACAM3 *in vitro*. To demonstrate that this interaction occurs in intact cells, we took advantage of FRET between closely opposed molecules. Therefore, the CEACAM3 cytoplasmatic domain was tagged with the FRET donor CyPet and the FRET acceptor YPet was fused to the amino-terminal SH2 domain of PI3K. We have previously shown that this pair of fluorophores can be used to detect FRET between CEACAM3 and associated proteins (26). Lysates were prepared from HEK293 cells expressing YPet-PI3K-N-SH2 together with CEACAM3 WT-CyPet, CEACAM3 ΔCT-CyPet, or CEACAM3 Y230F/Y241F-CyPet in the presence or absence of v-Src and expression of the proteins was verified by Western blotting (Fig. 4*A*). FRET between CyPet- and YPet-tagged proteins in the lysates was detected by measuring sensitized emission using a spectrofluorometer. As expected, an apparent FRET efficiency was only detectable in the case of phosphorylated CEACAM3 WT, but not in lysates containing CEACAM3 ΔCT or CEACAM3 Y230F/Y241F (Fig. 4*B*). Furthermore, the FRET signal was absent in cells harboring CEACAM3 WT, but lacking v-Src expression (Fig. 4*B*) demonstrating that YPet-PI3K-N-SH2 association with CEACAM3 WT-CyPet was dependent on phosphorylation of the cytoplasmatic domain. To confirm the specificity of the observed FRET signal we competed the interaction of CEACAM3-CyPet with YPet-PI3K-N-SH2 by addition of the recombinant unlabeled c-Src SH2 domain (GST-Src SH2) to the lysates. Indeed, GST-Src SH2 acted as a specific competitive inhibitor that displaced YPet-PI3K-N-SH2 from the receptor resulting in a strongly diminished FRET signal (Fig. 4*B*). In contrast, addition of GST did not affect FRET efficiency (data not shown). Similar results were obtained by a flow cytometry approach. In this regard, CyPet and YPet double-positive cells were gated and their fluorescence was analyzed in the FRET channel recording YPet emission (525/50 nm) upon excitation of CyPet at 405 nm. Cells expressing CEACAM3 ΔCT or expressing CEACAM3 WT in the absence of v-Src exhibit only a weak fluorescence signal, whereas cells co-expressing CEACAM3 WT and PI3K-N-SH2 in the presence of v-Src displayed a stronger signal in the FRET channel (Fig. 4, *C* and *D*). To finally corroborate the direct interaction between PI3K-N-SH2 and CEACAM3 at sites of bacterial-host cell contact we microscopically localized the FRET signal by acceptor photobleaching in infected cells. Therefore, HEK293 cells co-expressing CEACAM3 WT-CyPet and YPet-PI3K-N-SH2 were infected with AF647-labeled Opa_{52} protein expressing gonococci for 30 min and fixed. Images were recorded in all three fluorescence channels (Fig. 4*E*). Then, the acceptor fluorophore (YPet) was bleached in a defined region, where CEACAM3 was engaged by bacteria and co-localized with the SH2 domain of PI3K. In the case of FRET, bleaching of the acceptor fluorophore should result in an increased donor (CyPet) signal. Indeed, an increase in CyPet fluorescence was observed exactly at the point of contact between bacteria and the host receptor (Fig. 4, *E* and *F*). In contrast, bleached regions without bacteria or unbleached regions showed unaltered CyPet intensity (Fig. 4, *E* and *F*). Taken together these results demonstrate the direct association of the SH2 domain of PI3K with tyrosine-phosphorylated CEACAM3 in intact cells and localize this interaction to the sites of gonococcal-host cell contact.

PI 3-Kinase Activity Is Dispensable for CEACAM3-mediated Uptake of Bacteria—Given the specific recruitment of the PI3K regulatory subunit to CEACAM3 we wondered about the functional relevance of this protein-protein interaction. To interfere broadly with PI3K activity in CEACAM3-mediated uptake, we applied pharmacological PI3K inhibitors. Unexpectedly, uptake of the Opa_{52} protein expressing gonococci by CEACAM3-expressing HEK293 cells was unaltered in the presence of different concentrations of wortmannin (Fig. 5*A*). CEACAM3 is exclusively expressed by human granulocytes and mediates opsonin-independent uptake of CEACAM-binding bacteria (23). Therefore, we treated primary human granulocytes with two different PI 3-kinase inhibitors prior to infection with fluorescein-labeled gonococci. Phagocytosis of the bacteria was analyzed by a flow cytometric method that quantifies intracellular bacteria (37). Importantly, pretreatment of granulocytes with wortmannin concentrations up to 200 nM or with the inhibitor LY294002 up to 50 μM had no influence on bacterial internalization in agreement with the results obtained with HEK293 cells (Fig. 5*B*). As PI3Ks have been demonstrated to be crucial for FcγR-mediated uptake of Ig-opsonized bacteria in mouse macrophages, we verified that this process was sensitive to wortmannin in the used concentration range (Fig. 5*C*). Interestingly, phagocytosis of Ig-opsonized non-opaque gonococci by human granulocytes was independent of PI3K activity suggesting that not only differences in the involved phagocytic receptors, but also the cell type might determine

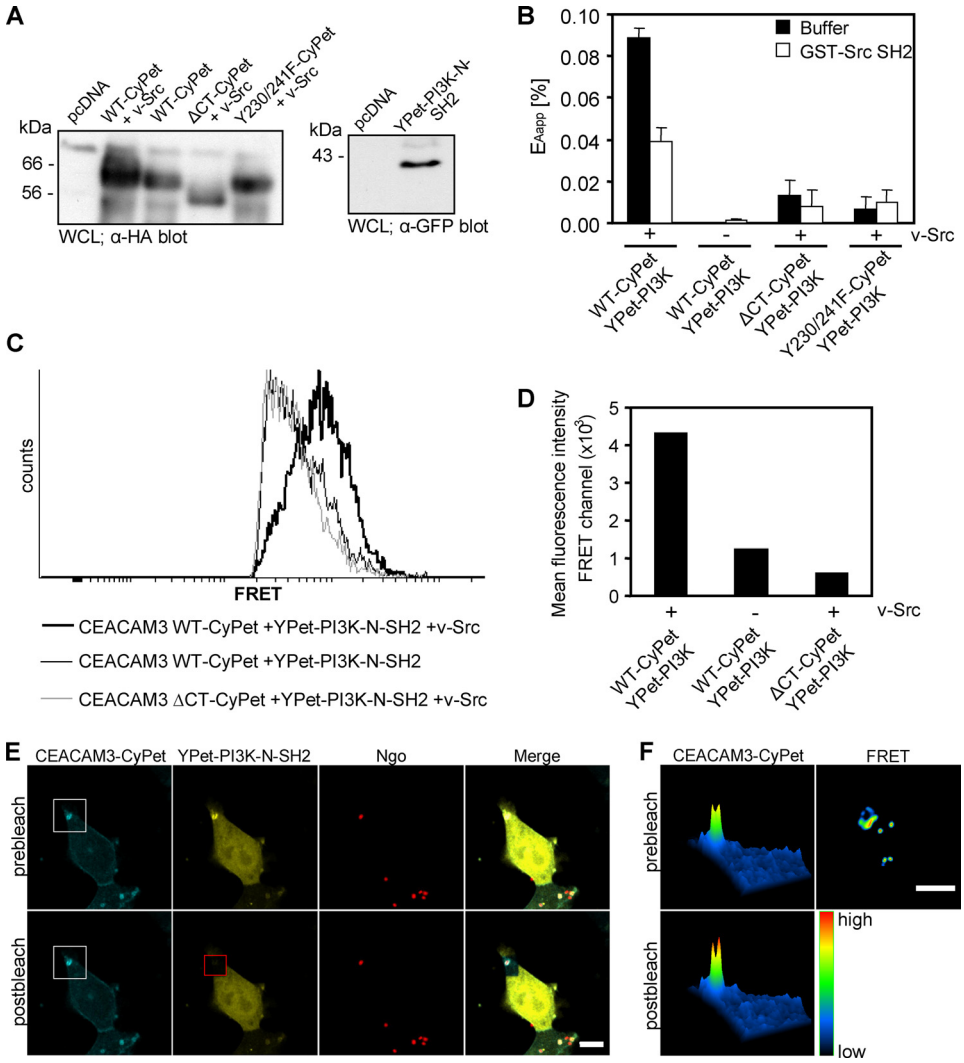

FIGURE 4. **PI3K-N-SH2 interacts with phosphorylated ITAM-like sequence of CEACAM3 *in vivo*.** *A*, HEK293 cells were cotransfected to express a HA-tagged CyPet fusion protein of wild type CEACAM3 (*WT-CyPet*), truncated CEACAM3 (Δ*CT-CyPet*), or a tyrosine mutant of CEACAM3 (*Y230F/Y241F-CyPet*) together with YPet-PI3K-N-SH2 and v-Src as indicated. Cells were lysed 2 days after transfection. Expression of the proteins was confirmed by Western blotting of whole cell lysates (*WCL*) with anti-HA antibodies (*left panel*) or anti-GFP antibodies (*right panel*). *B*, fluorescence of the lysates from *A* was determined separately in the donor, acceptor, and FRET channel, respectively, and apparent FRET efficiency ($E_{A(app)}$; *black bars*) was calculated. Purified GST-Src-SH2 was added to the lysates as a competitive inhibitor of YPet-PI3K-N-SH2 and measurements were repeated (*open bars*). *Bars* represent mean ± S.E. of three independent experiments. *C*, HEK293 cells were transfected as indicated. Two days after transfection, double positive cells were identified by flow cytometry and analyzed for FRET. The histogram depicts the fluorescence intensity distribution in the FRET channel. *D*, mean fluorescence intensity in the FRET channel derived from the histogram in *C*. *E*, HEK293 cells were cotransfected to express wild type CEACAM3 (*CEACAM3-CyPet*) and YPet-PI3K-N-SH2. Two days later cells were infected with AF647-labeled Opa_{52} protein-expressing gonococci (*Ngo*) for 30 min and fixed. Images were recorded before and after photobleaching the YPet acceptor in a defined region around CEACAM3-bound bacteria (*red rectangle*). *Scale bar*, 10 μm. *F*, surface plot of the *white marked region* in *E* including the bleached area. FRET was calculated as described under "Experimental Procedures." Images are presented in pseudo-color for better visualization. *Scale bar*, 5 μm.

wortmannin sensitivity of this process (Fig. 5*D*). Clearly, CEACAM3-binding bacteria led to the local recruitment of PI 3-kinase within 15 min after contact with human granulocytes (Fig. 5*E*). In contrast, only small numbers of non-opaque gonococci were phagocytosed by human granulocytes in the absence of opsonization (Fig. 5*B*) and they did not lead to PI 3-kinase recruitment (Fig. 5*E*).

PI 3-Kinase Activity Is Critical for an Oxidative Burst and Bacterial Destruction during CEACAM3-initiated Phagcytosis—The products of PI3K activity are also involved in regulating the assembly of a functional NADPH oxidase complex in phagocytes (40). Therefore, we measured the production of reactive oxygen species by human granulocytes in response to CEACAM-binding bacteria. In the absence of opsonizing agents such as specific antibodies or complement, non-opaque gonococci did not trigger an oxidative response by unstimulated granulocytes, whereas Opa_{52} protein expressing bacteria triggered a strong oxidative response (Fig. 6, *A* and *B*). Interestingly, gonococci expressing the CEACAM1 and CEA-binding Opa_{56} protein, which does not engage CEACAM3 (16) (Fig. 6*C*) and does not induce uptake by human primary granulocytes (Fig. 6*D*), did not trigger an oxidative burst in primary granulocytes (Fig. 6, *A* and *B*). Treatment of granulocytes with wortmannin reduced the oxidative response in a dose-dependent manner, and at concentrations as low as 10 nM wortmannin the generation of reactive oxygen species was completely abolished (Fig. 6*E* and supplemental Fig. S1). These results suggest that the rapid recruitment and activation of PI3K in response to

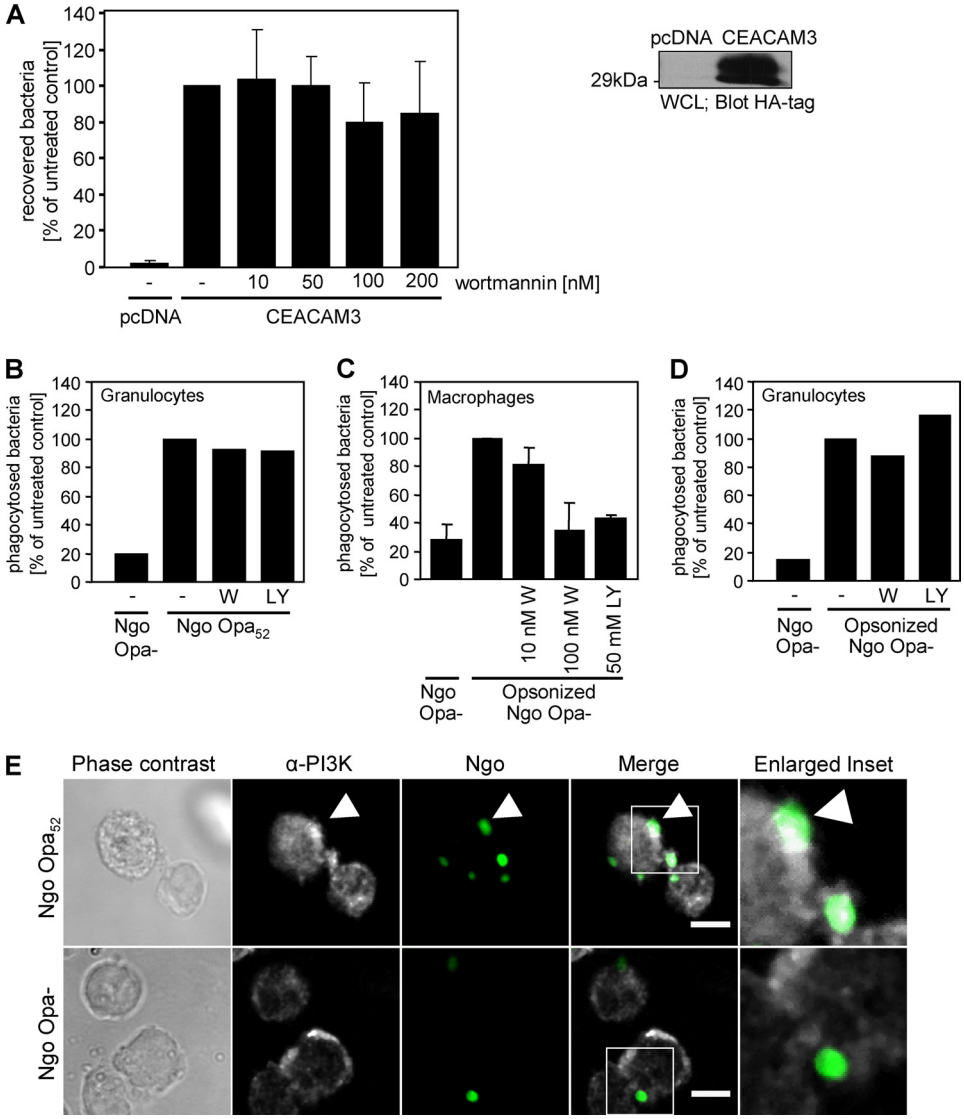

FIGURE 5. **PI 3-kinase activity is dispensable for CEACAM3-mediated bacterial uptake.** *A*, HEK293 cells were transfected with HA-tagged wild type CEACAM3 or the empty control vector (*pcDNA*) and employed in gentamicin protection assays. Cells were pretreated with different concentrations of wortmannin for 30 min before infection with Opa_{52} protein-expressing gonococci (m.o.i. 30) for 1 h. The graph shows mean ± S.D. of four independent experiments done in triplicate. Western blot of whole cell lysates (*WCL*) confirmed expression of CEACAM3 in HEK293 cells (*right panel*). *B*, human primary granulocytes were incubated with wortmannin (*W*; 200 nM) or LY294002 (*LY*; 50 μM). Granulocytes were infected with fluorescein-labeled non-opaque gonococci (*Ngo Opa*−), Opa_{52} protein expressing (*Ngo* Opa_{52}) gonococci (m.o.i. 25), or left uninfected. After 15 min, phagocytosis was measured by flow cytometry. Fluorescence of extracellular, adherent bacteria was quenched by addition of trypan blue. The graph is derived from a representative experiment. Equivalent results were obtained with granulocytes isolated from three different donors. *C*, raw 264.7 mouse macrophages were preincubated with the indicated concentrations of wortmannin (*W*) and infected with opsonized fluorescein-labeled non-opaque gonococci (m.o.i. 50). After 30 min phagocytosis was quantified as in *B*. *Bars* represent mean ± S.D. from three independent experiments. *D*, human granulocytes were incubated with 100 nM wortmannin (*W*) or 50 μM LY294002 (*LY*) and infected with opsonized fluorescein-labeled non-opaque gonococci (m.o.i. 50). After 15 min phagocytosis was quantified as in *B*. The graph shows values from a representative experiment. Equivalent results were obtained with granulocytes isolated from three different donors. *E*, PI 3-kinase is recruited to sites of bacterial infection. Human granulocytes were infected with Pacific Blue-labeled Opa_{52} protein-expressing (*Ngo* Opa_{52}) or non-opaque (*Ngo Opa*−) gonococci (m.o.i. 30) for 15 min and fixed. PI3K was visualized after cell permeabilization by using a polyclonal anti-PI3K Ab and a Cy3-conjugated goat anti-rabbit Ab. *Scale bars*, 5 μm.

bacterial engagement of CEACAM3 is instrumental for stimulating the generation of reactive oxygen species.

To address if this PI3K-dependent bactericidal response allows the killing and destruction of internalized bacteria, we infected primary granulocytes at a low m.o.i. of one bacterium per cell. 60 or 240 min after infection, samples were lysed and probed for the presence of intact gonococcal Opa protein. In the case of Opa_{56} protein expressing bacteria, which were not recognized by CEACAM3 and which did not trigger an oxidative burst, the Opa protein could be detected at both time points (Fig. 6*F*). In contrast, the CEACAM3-binding Opa_{52} protein was almost completely degraded after 240 min suggesting that the bacteria in this sample had been phagocytosed and destroyed (Fig. 6*F*). Addition of trypsin to bacterial suspensions demonstrated that both, the Opa_{52} and Opa_{56} proteins were equally sensitive to protease treatment (Fig. 6*G*). Most importantly, degradation of the Opa_{52} protein by human granulocytes was inhibited by wortmannin demonstrating that CEACAM3-triggered PI3K activity, presumably by promoting the oxidative burst, allows rapid destruction of the internalized bacteria (Fig.

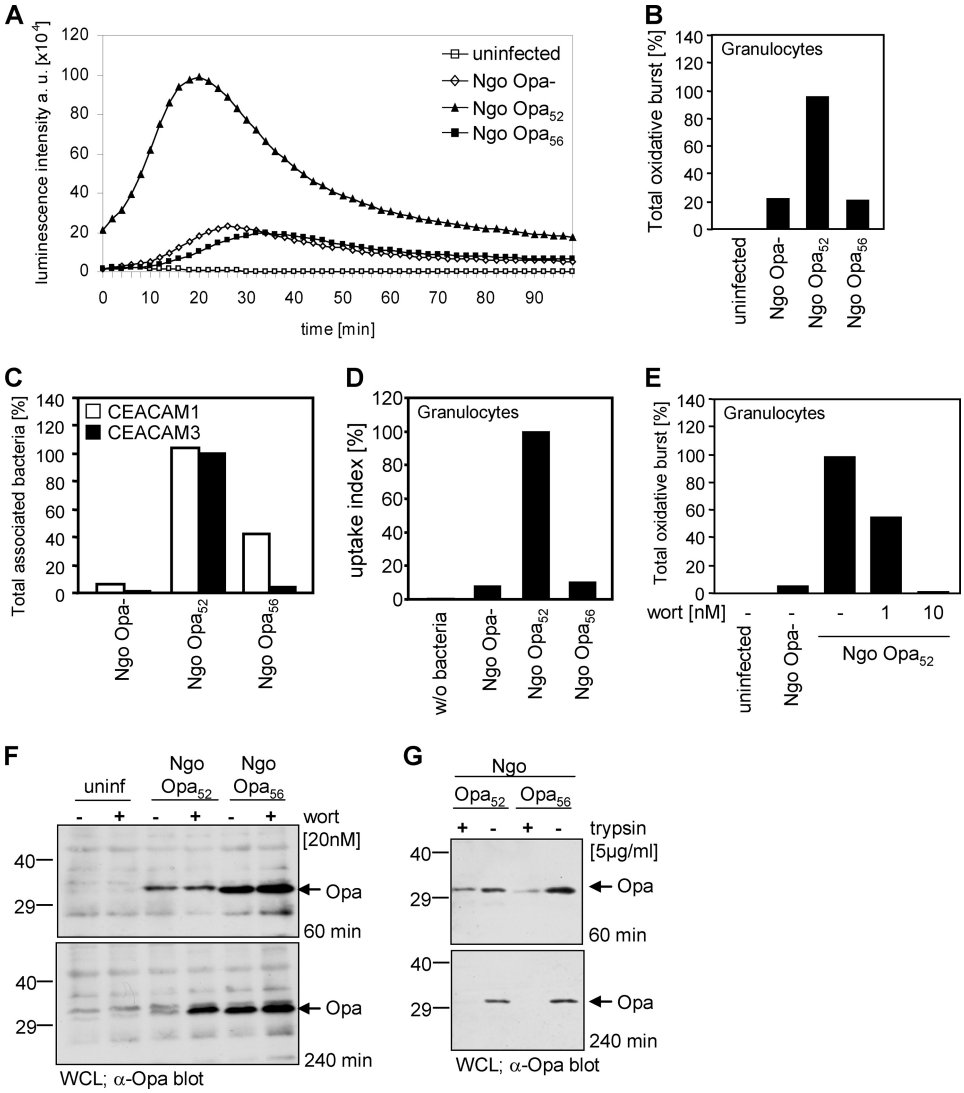

FIGURE 6. **PI 3-kinase activity is critical for the granulocyte oxidative burst and intracellular destruction of gonococci following CEACAM3-mediated phagocytosis.** *A*, primary human granulocytes were infected at an m.o.i. of 50 with non-opaque gonococci (*Ngo Opa*−), Opa_{52} protein expressing gonococci (*Ngo* Opa_{52}), Opa_{56} protein-expressing gonococci (*Ngo* Opa_{56}), or left uninfected and the oxidative burst was measured for 100 min. The graph shows a representative experiment. Similar results were obtained with granulocytes from three different donors. *B*, oxidative burst was measured as described in *A*. To determine the total oxidative burst, the area *under* the curves was calculated. The graph shows a representative experiment. Similar results were obtained with granulocytes from three different donors. *C*, HEK293 cells were transfected with either a CEACAM1-mKate (*white bars*) or a CEACAM3-mKate (*black bars*) encoding construct. Cells were infected with fluorescein-labeled Ngo Opa−, Ngo Opa_{52}, or Ngo Opa_{56}, respectively, at an m.o.i. 20 for 180 min. Using flow cytometry, the mKate-positive cells were identified and the associated, fluorescein-positive bacteria were quantified. Results are from a representative experiment. Equivalent results were obtained in two independent repetitions. *D*, human granulocytes were infected with fluorescein-labeled Ngo Opa−, Ngo Opa_{52}, Ngo Opa_{56} (m.o.i. 25), or left uninfected. After 15 min, phagocytosis was measured by flow cytometry. Fluorescence of extracellular, adherent bacteria was quenched by addition of trypan blue. The graph is derived from a representative experiment. Equivalent results were obtained with granulocytes isolated from three different donors. *E*, granulocytes were pretreated with the indicated concentrations of wortmannin. Cells were left uninfected or infected with Ngo Opa− or Ngo Opa_{52} and the oxidative burst was measured and quantified as in *B*. The graph shows a representative experiment. Similar results were obtained with granulocytes from three different donors. *F*, human granulocytes were infected with Ngo Opa_{52} or Ngo Opa_{56} (m.o.i. 1) for 60 and 240 min in the presence or absence of wortmannin. Degradation of Opa proteins was analyzed in whole cell lysates (*WCL*) by Western blotting with a monoclonal anti-Opa antibody. *G*, gonococci expressing Opa_{52} or Opa_{56} were incubated in the presence or absence of trypsin for 60 and 240 min. Degradation of Opa proteins was analyzed as in *F*.

6*F*). Together, these results suggest that the CEACAM3-initiated recruitment and activation of PI3K is not only instrumental for stimulating the generation of reactive oxygen species, but also for the efficient elimination of CEACAM-binding bacteria by human granulocytes.

DISCUSSION

Several human-adapted bacterial pathogens exploit members of the CEACAM family to colonize the mucosal surface of their host. In turn, the human innate immune system is equipped with a dedicated phagocytic receptor, CEACAM3, that allows the opsonin-independent recognition of CEACAM-binding bacteria.

Here we show that the granulocyte receptor CEACAM3 not only mediates binding and phagocytosis of bacterial pathogens, but also initiates a bactericidal oxidative burst. The rapid generation of reactive oxygen intermediates by granulocytes in response to CEACAM-binding microbes depends on the activity of PI3K that is recruited to clustered CEACAM3. SH2

domain-mediated direct association of the regulatory subunit of PI3K with phospho-Tyr^{230} of the CEACAM3 ITAM-like sequence explains the speed and efficiency of the granulocyte oxidative response toward non-opsonized CEACAM3-binding *N. gonorrhoeae* and suggests that CEACAM3-mediated innate immune responses help to limit the spread of CEACAM-binding bacteria in their human host.

Interestingly, phosphorylated tyrosine residue 230 ($Tyr(P)^{230}$) within the ITAM-like sequence of CEACAM3 has also been found to serve as a binding site for the guanine nucleotide exchange factor Vav (30). Furthermore, Tyr^{230} is embedded in a Y*XX*L motif that has been shown to be a target for the SH2 domains of the Src family PTKs (41). Indeed, we have observed that the well documented interaction between CEACAM3 and Src family PTKs such as Hck and Yes also takes place at this tyrosine residue (21, 26).[4] To explain the association of a single amino acid residue with multiple factors critical for CEACAM3-induced signaling, there are several, non-exclusive possibilities. On the one hand, the multivalent bacteria clearly trigger the clustering of multiple CEACAM3 molecules in a locally confined region of the cell (23, 26). It is therefore possible that all $Tyr(P)^{230}$-binding components bind at the same time and accumulate in the same region of the cell. In such a case, a fraction of the phosphorylated receptors could be occupied with a given SH2-domain containing protein, where the size of the fraction would be determined by the binding affinity and local concentrations compared with other binding partners. On the other hand, the association between the cytoplasmic domain of CEACAM3 and cytoplasmic binding partners is transient. Live cell imaging has revealed that following CEACAM3 engagement and clustering by Opa_{CEA}-protein expressing *N. gonorrhoeae*, the Hck SH2 domain is rapidly recruited and then disappears again from the receptor within 5–10 min (26). Accordingly, there might be a hierarchy of cytoplasmic factors that associate with the CEACAM3 cytoplasmic domain in a temporally ordered fashion. Further analysis by live cell microscopy using differentially tagged SH2 domains as well as additional biochemical analysis of dissociation constants between CEACAM3 and a panel of SH2 domains will clarify the contribution of each of these mechanisms to CEACAM3 signaling.

A surprising result of our studies is the finding that the recruitment and the direct association with PI3K seem to be dispensable for CEACAM3-initiated phagocytosis of bacteria. Clearly, PI3K activity is not needed for bacterial uptake, neither in CEACAM3-transfected cell lines, nor in primary human granulocytes, where this receptor is endogenously expressed. These results are in strong contrast to the documented essential role of PI3K activity during opsonin-mediated uptake of particles via the Fcγ receptor (42). Similar to CEACAM3, FcγRIIa is a single-chain phagocytic receptor that bears a canonical ITAM motif in its cytoplasmic domain, whereas FcγRI and FcγRIII require co-expression of a separate ITAM containing γ-chain to mediate particle uptake (28). When functional FcγRs are expressed in non-professional phagocytes, phagocytosis of IgG-opsonized red blood cells (IgG-RBC) is highly sensitive to wortmannin treatment with an IC_{50} of 8 nM (28). It has been observed that inhibition by wortmannin depends on particle size, as IgG-opsonized latex beads below 2 μm can be taken up by a PI3K-independent pathway (43). Usually, diplococcal *N. gonorrhoeae* has a size around 1–2 μm suggesting that this bacterium could be below the critical size for PI3K-dependent uptake. However, our experiments with murine macrophages and human granulocytes reveal that IgG-opsonized gonococci are internalized in a mechanistically distinct manner by the two cell types. Obviously, in this case it is not only the size or opsonization of the microbial particle, but also the cell type that determines if the uptake occurs in a PI3K-dependent or -independent manner. Clearly, opsonin-independent CEACAM3-mediated internalization of the Opa_{CEA} protein expressing gonococci by human granulocytes does not require PI3K activity.

Our results of a PI3K-independent uptake of Opa_{CEA}-expressing *N. gonorrhoeae* are on first sight in conflict with a previous report showing that the ratio of internalized *versus* cell-associated gonococci is reduced about 40% in the presence of wortmannin (34). However, because the number of cell-associated bacteria in that experimental system is increased about 50% by wortmannin treatment (see Fig. 2) (34), the absolute number of internalized gonococci is unaltered in the presence of wortmannin. In our investigation, we have not observed an alteration in total cell-associated bacteria, neither in CEACAM3-transfected HEK293 cells nor in primary human granulocytes upon inhibition of PI3K suggesting that the discrepancy might be a result of the microscopic evaluation of bacterial internalization in a small number of cells used previously.

Despite the fact that PI3K activity is obsolete for the CEACAM3-mediated uptake of Opa_{CEA} protein expressing *N. gonorrhoeae*, the direct association of the clustered receptor with the regulatory subunit of PI3K will position this lipid kinase close to its membrane substrate. Indeed, a strong increase in PI(3,4,5)P levels in the vicinity of CEACAM3-associated bacteria has been observed by the specific recruitment of fluorescently labeled PH domains (34). Besides the re-organization of the actin cytoskeleton due to the recruitment of guanine nucleotide exchange factors for Rho GTPases such as Vav or Tiam or the activation of kinases such as PKB or Tec, PI(3,4,5)P also has a central role in regulating effector functions of granulocytes (44–46). In particular, the neutrophil NADPH oxidase complex consisting of two membrane-bound subunits (cytochrome b_{558}/$gp91^{phox}$ and $p22^{phox}$) and four soluble proteins ($p67^{phox}$, $p47^{phox}$, $p40^{phox}$, and GTP-loaded Rac2) is tightly regulated and requires input by 3′-phosphorylated phosphatidylinositides at multiple stages (40, 47). For example, membrane translocation and activation of the Rac2 guanine nucleotide exchange factor P-Rex1 requires PI(3,4,5)P (48, 49). Furthermore, PI(3,4,5)P can be turned over by lipid phosphatases to generate PI3P, which is also produced by class III phosphatidylinositol 3′-kinases (50). PI3P is critical for the recruitment and allosteric activation of $p40^{phox}$, a process that is involved in FcγR-induced production of reactive oxygen species (51, 52). As wortmannin and LY294002 inhibit class I as

[4] K. Kopp, R. Frank, and C. R. Hauck, unpublished observations.

well as class III phosphatidylinositol 3′-kinases, it is not possible to judge the contribution of each of these enzyme classes for CEACAM3-initiated reactive oxygen species formation. However, it seems feasible that maximal activation of NADPH oxidase in response to CEACAM3-binding bacteria requires a coordinated action of both classes of phosphatidylinositol 3′-kinases. Clearly, the activity of PI3K was instrumental for the intracellular destruction of the phagocytosed bacteria within a few hours, pointing to coordinated processing of internalized gonococci by reactive oxygen derivatives and host proteolytic enzymes.

Interestingly, besides *N. gonorrhoeae* several other Gram-negative, human-adapted pathogens possess CEACAM-binding adhesins including *N. meningitidis*, *Haemophilus influenzae*, and *Moraxella catarrhalis* (53). Similar to gonococci, these pathogens are able to evade acquired immune responses by different mechanisms including secretion of immunoglobulin-cleaving proteases or variation of surface components. CEACAM3 expression by granulocytes appears as a specific adaptation of the human innate immune system to employ a germ-line encoded receptor for efficient phagocytosis and killing of CEACAM-binding bacteria. The results of our study underscore that the molecular connections of the ITAM-like sequence in the cytoplasmic domain of CEACAM3 are critical to coordinate these processes, and provide impetus for further analysis of this specific phagocytic receptor.

Acknowledgments—We thank T. F. Meyer (MPI for Infection Biology, Berlin, Germany) for the Neisseria strains used in this study, Patrick Daugherty (University of California, Santa Barbara, CA) for CyPet and YPet cDNAs, Dmitriy Chudakov (Shemyakin and Ovchinnikov Institute of Bioorganic Chemistry, Moscow, Russia) for mKate cDNA, and R. Hohenberger-Bregger, S. Feindler-Boeckh, and S. Daenicke for expert technical assistance.

REFERENCES

1. Marrazzo, J. M., Handsfield, H. H., and Sparling, P. F. (2010) in *Principles and Practice of Infectious Diseases* (Mandell, G. L., Bennett, J. E., and Dolin, R., eds) pp. 2753–2770, Churchill Livingstone, Philadelphia, PA
2. Meyer, T. F., Gibbs, C. P., and Haas, R. (1990) *Annu. Rev. Microbiol.* **44,** 451–477
3. Hauck, C. R., and Meyer, T. F. (2003) *Curr. Opin. Microbiol.* **6,** 43–49
4. Stern, A., Brown, M., Nickel, P., and Meyer, T. F. (1986) *Cell* **47,** 61–71
5. Kuespert, K., Pils, S., and Hauck, C. R. (2006) *Curr. Opin. Cell Biol.* **18,** 565–571
6. Chen, T., and Gotschlich, E. C. (1996) *Proc. Natl. Acad. Sci. U.S.A.* **93,** 14851–14856
7. Virji, M., Watt, S. M., Barker, S., Makepeace, K., and Doyonnas, R. (1996) *Mol. Microbiol.* **22,** 929–939
8. Voges, M., Bachmann, V., Kammerer, R., Gophna, U., and Hauck, C. R. (2010) *BMC Microbiol.* **10,** 117
9. Zebhauser, R., Kammerer, R., Eisenried, A., McLellan, A., Moore, T., and Zimmermann, W. (2005) *Genomics* **86,** 566–580
10. Virji, M., Makepeace, K., Ferguson, D. J., and Watt, S. M. (1996) *Mol. Microbiol.* **22,** 941–950
11. Chen, T., Grunert, F., Medina-Marino, A., and Gotschlich, E. C. (1997) *J. Exp. Med.* **185,** 1557–1564
12. Gray-Owen, S. D., Lorenzen, D. R., Haude, A., Meyer, T. F., and Dehio, C. (1997) *Mol. Microbiol.* **26,** 971–980
13. Bos, M. P., Kuroki, M., Krop-Watorek, A., Hogan, D., and Belland, R. J. (1998) *Proc. Natl. Acad. Sci. U.S.A.* **95,** 9584–9589
14. Popp, A., Dehio, C., Grunert, F., Meyer, T. F., and Gray-Owen, S. D. (1999) *Cell. Microbiol.* **1,** 169–181
15. Kuespert, K., Weibel, S., and Hauck, C. R. (2007) *J. Microbiol. Methods* **68,** 478–485
16. Bos, M. P., Grunert, F., and Belland, R. J. (1997) *Infect. Immun.* **65,** 2353–2361
17. Muenzner, P., Rohde, M., Kneitz, S., and Hauck, C. R. (2005) *J. Cell Biol.* **170,** 825–836
18. Muenzner, P., Bachmann, V., Zimmermann, W., Hentschel, J., and Hauck, C. R. (2010) *Science* **329,** 1197–1201
19. Pils, S., Gerrard, D., Meyer, A., and Hauck, C. R. (2008) *Intl. J. Med. Microbiol.* **298,** 553–560
20. McCaw, S. E., Liao, E. H., and Gray-Owen, S. D. (2004) *Infect. Immun.* **72,** 2742–2752
21. Schmitter, T., Pils, S., Weibel, S., Agerer, F., Peterson, L., Buntru, A., Kopp, K., and Hauck, C. R. (2007) *Infect. Immun.* **75,** 4116–4126
22. Muenzner, P., Bachmann, V., Kuespert, K., and Hauck, C. R. (2008) *Cell. Microbiol.* **10,** 1074–1092
23. Schmitter, T., Agerer, F., Peterson, L., Munzner, P., and Hauck, C. R. (2004) *J. Exp. Med.* **199,** 35–46
24. Hauck, C. R., Meyer, T. F., Lang, F., and Gulbins, E. (1998) *EMBO J.* **17,** 443–454
25. McCaw, S. E., Schneider, J., Liao, E. H., Zimmermann, W., and Gray-Owen, S. D. (2003) *Mol. Microbiol.* **49,** 623–637
26. Buntru, A., Zimmermann, T., and Hauck, C. R. (2009) *BMC Biol.* **7,** 81
27. Billker, O., Popp, A., Brinkmann, V., Wenig, G., Schneider, J., Caron, E., and Meyer, T. F. (2002) *EMBO J.* **21,** 560–571
28. Indik, Z. K., Park, J. G., Hunter, S., and Schreiber, A. D. (1995) *Blood* **86,** 4389–4399
29. Sarantis, H., and Gray-Owen, S. D. (2007) *Cell. Microbiol.* **9,** 2167–2180
30. Schmitter, T., Pils, S., Sakk, V., Frank, R., Fischer, K. D., and Hauck, C. R. (2007) *J. Immunol.* **178,** 3797–3805
31. Hall, A. B., Gakidis, M. A., Glogauer, M., Wilsbacher, J. L., Gao, S., Swat, W., and Brugge, J. S. (2006) *Immunity* **24,** 305–316
32. Piccione, E., Case, R. D., Domchek, S. M., Hu, P., Chaudhuri, M., Backer, J. M., Schlessinger, J., and Shoelson, S. E. (1993) *Biochemistry* **32,** 3197–3202
33. Cullen, P. J., Cozier, G. E., Banting, G., and Mellor, H. (2001) *Curr. Biol.* **11,** R882–893
34. Booth, J. W., Telio, D., Liao, E. H., McCaw, S. E., Matsuo, T., Grinstein, S., and Gray-Owen, S. D. (2003) *J. Biol. Chem.* **278,** 14037–14045
35. Hauck, C. R., Hunter, T., and Schlaepfer, D. D. (2001) *J. Biol. Chem.* **276,** 17653–17662
36. Kupsch, E. M., Knepper, B., Kuroki, T., Heuer, I., and Meyer, T. F. (1993) *EMBO J.* **12,** 641–650
37. Pils, S., Schmitter, T., Neske, F., and Hauck, C. R. (2006) *J. Microbiol. Methods* **65,** 301–310
38. Swanson, J. A., and Hoppe, A. D. (2004) *J. Leukocyte Biol.* **76,** 1093–1103
39. Frank, R. (1992) *Tetrahedron* **48,** 9217–9232
40. Hawkins, P. T., Davidson, K., and Stephens, L. R. (2007) *Biochem. Soc. Symp.* **74,** 59–67
41. Songyang, Z., Shoelson, S. E., Chaudhuri, M., Gish, G., Pawson, T., Haser, W. G., King, F., Roberts, T., Ratnofsky, S., Lechleider, R. J., *et al.* (1993) *Cell* **72,** 767–778
42. Araki, N., Johnson, M. T., and Swanson, J. A. (1996) *J. Cell Biol.* **135,** 1249–1260
43. Cox, D., Tseng, C. C., Bjekic, G., and Greenberg, S. (1999) *J. Biol. Chem.* **274,** 1240–1247
44. Dewald, B., Thelen, M., and Baggiolini, M. (1988) *J. Biol. Chem.* **263,** 16179–16184
45. Arcaro, A., and Wymann, M. P. (1993) *Biochem. J.* **296,** 297–301
46. Hawkins, P. T., Anderson, K. E., Davidson, K., and Stephens, L. R. (2006) *Biochem. Soc. Trans.* **34,** 647–662
47. Bokoch, G. M., and Diebold, B. A. (2002) *Blood* **100,** 2692–2696
48. Zhao, T., Nalbant, P., Hoshino, M., Dong, X., Wu, D., and Bokoch, G. M. (2007) *J. Leukocyte Biol.* **81,** 1127–1136
49. Welch, H. C., Coadwell, W. J., Ellson, C. D., Ferguson, G. J., Andrews, S. R.,

Erdjument-Bromage, H., Tempst, P., Hawkins, P. T., and Stephens, L. R. (2002) *Cell* **108,** 809–821
50. Vanhaesebroeck, B., Leevers, S. J., Ahmadi, K., Timms, J., Katso, R., Driscoll, P. C., Woscholski, R., Parker, P. J., and Waterfield, M. D. (2001) *Annu. Rev. Biochem.* **70,** 535–602
51. Ellson, C., Davidson, K., Anderson, K., Stephens, L. R., and Hawkins, P. T. (2006) *EMBO J.* **25,** 4468–4478
52. Suh, C. I., Stull, N. D., Li, X. J., Tian, W., Price, M. O., Grinstein, S., Yaffe, M. B., Atkinson, S., and Dinauer, M. C. (2006) *J. Exp. Med.* **203,** 1915–1925
53. Gray-Owen, S. D., and Blumberg, R. S. (2006) *Nat. Rev. Immunol.* **6,** 433–446